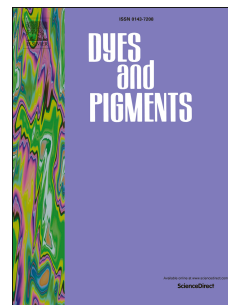


Journal Pre-proof

Versatile thiopyridyl/pyridinone porphyrins combined with potassium iodide and thiopyridinium/methoxythiopyridinium porphyrins on *E. coli* photoinactivation

Joana M.D. Calmeiro, Sara R.D. Gamelas, Ana T.P.C. Gomes, Maria A.F. Faustino, Maria G.P.M.S. Neves, Adelaide Almeida, João P.C. Tomé, Leandro M.O. Lourenço



PII: S0143-7208(20)30499-X

DOI: <https://doi.org/10.1016/j.dyepig.2020.108476>

Reference: DYPI 108476

To appear in: *Dyes and Pigments*

Received Date: 21 February 2020

Revised Date: 2 April 2020

Accepted Date: 23 April 2020

Please cite this article as: Calmeiro JMD, Gamelas SRD, Gomes ATPC, Faustino MAF, Neves MGPMS, Almeida A, Tomé JoãPC, Lourenço LMO, Versatile thiopyridyl/pyridinone porphyrins combined with potassium iodide and thiopyridinium/methoxythiopyridinium porphyrins on *E. coli* photoinactivation, *Dyes and Pigments* (2020), doi: <https://doi.org/10.1016/j.dyepig.2020.108476>.

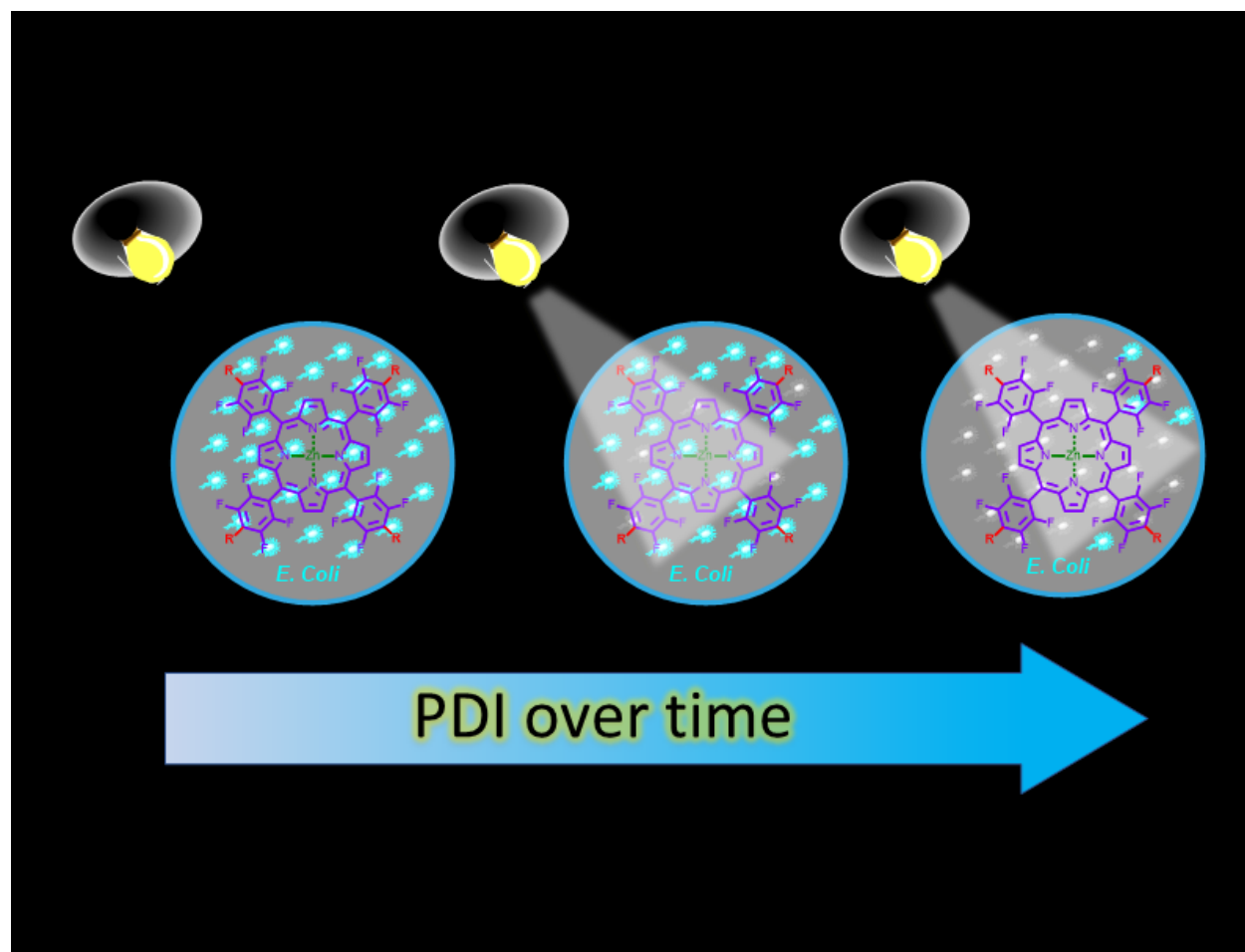
This is a PDF file of an article that has undergone enhancements after acceptance, such as the addition of a cover page and metadata, and formatting for readability, but it is not yet the definitive version of record. This version will undergo additional copyediting, typesetting and review before it is published in its final form, but we are providing this version to give early visibility of the article. Please note that, during the production process, errors may be discovered which could affect the content, and all legal disclaimers that apply to the journal pertain.

© 2020 Published by Elsevier Ltd.

Sample CRediT author statement:

Joana M. D. Calmeiro: Writing - Original Draft, Conceptualization, Validation. **Sara R. D. Gamas:** Writing - Original Draft, Conceptualization, Validation. **Ana T. P. C. Gomes:** Writing - Review & Editing, Supervision, Methodology, Validation. **Maria A. F. Faustino:** Writing - Review & Editing, Visualization, Validation. **Maria G. P. M. S. Neves:** Writing - Review & Editing, Conceptualization, Visualization. **Adelaide Almeida:** Writing - Review & Editing, Resources, Validation, Funding acquisition. **João P. C. Tomé:** Writing - Review & Editing, Visualization, Validation. **Leandro M. O. Lourenço:** Writing - Review & Editing, Validation, Supervision, Funding acquisition.

Journal Pre-proof



Versatile thiopyridyl/pyridinone porphyrins combined with potassium iodide and thiopyridinium/methoxypyridinium porphyrins on *E. coli* photoinactivation

Joana M. D. Calmeiro,^{a,‡} Sara R. D. Gamelas,^{a,‡} Ana T. P. C. Gomes,^{b,*} Maria A. F. Faustino,^a Maria G. P. M. S. Neves,^a Adelaide Almeida,^b João P. C. Tomé,^c Leandro M. O. Lourenço^{a,*}

^aLAQV-REQUIMTE and Department of Chemistry, University of Aveiro, 3810-193 Aveiro, Portugal.

^bCESAM and Department of Biology, University of Aveiro, 3810-193 Aveiro, Portugal.

^cCentro de Química Estrutural and Departamento de Engenharia Química, Instituto Superior Técnico, Universidade de Lisboa, 1049-001 Lisboa, Portugal.

[‡] These authors contributed equally to this work.

Abstract

Porphyrins (Pors) are well-known photoactive molecules with recognized features to be explored as photosensitisers in the photodynamic inactivation (PDI) of microorganisms. The use of appropriate moieties like pyridinium groups is a remarkable strategy to add peripheral and internal positive charges in the Por structure making them more effective PSs against Gram-negative bacteria like *Escherichia coli* (*E. coli*). In this context, an easy synthetic access to obtain cationic Zn(II) porphyrins bearing thiopyridinium and inverted methoxypyridinium units (ZnPors **1c** and **2c**) was developed and their photo-physical and photo-chemical properties were evaluated. The photodynamic effectiveness of these complexes against a *E. coli* strain was also studied and compared with the efficacy of the corresponding free-bases (Pors **1b** and **2b**) and of the neutral precursors (Pors **1**, **1a**, **2**, **2a**), these last ones in the absence and in the presence of potassium iodide salt (KI). The obtained results demonstrate high PDI efficiency with the cationic free-base **1b** and the ZnPor **2c**; both derivatives were able to photoinactivate *E. coli* till the detection limit of the method at a concentration of 1.0 μM after 20 and 15 min of white light irradiation (25 $\text{mW}\cdot\text{cm}^{-2}$), respectively. Interestingly, under the same experimental conditions (1.0 μM and white light), the neutral Pors (**1**, **1a**, **2** and **2a**) with addition of KI salt show a fast inactivation rate, reaching the detection limit of the method after 5 min of irradiation.

1. Introduction

The increase and the incorrect use of antibiotics has led to an unintentional selective process of the microbial population resistant to the action of several antibiotics.¹ The growth number of resistant bacterial strains promoted a fast replication of this population and also the ability of developing mutations which can turn a microorganism to survive in the presence of antibiotics.^{2,3} This microbial mutation has led the scientific community to increase efforts to find efficient alternatives against this resistance to the antimicrobial agents.²⁻⁵

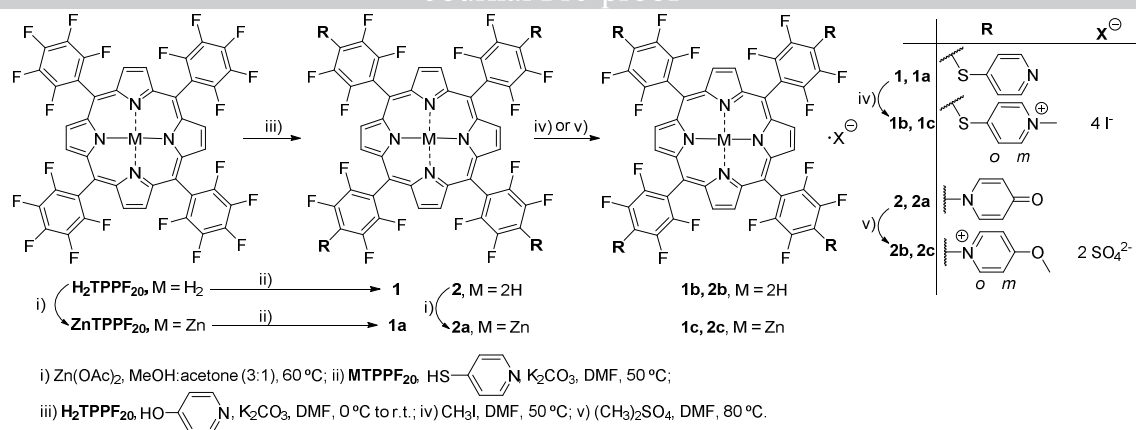
Photodynamic inactivation (PDI) of microorganisms emerges as an efficient alternative methodology to conventional therapeutic strategies. The combination of light irradiation, molecular oxygen and a photosensitizer (PS) produces reactive oxygen species (ROS), such as singlet oxygen ($^1\text{O}_2$) and free radicals, that are cytotoxic against several pathogenic microbial agents, such as: bacteria, viruses, fungi and protozoa.⁶⁻⁸ One of the main focus of PDI research is related with the development of promising PSs that can kill rapidly and efficiently microorganisms under white light irradiation.^{8,9} PSs, namely porphyrin (Por),¹⁰⁻¹⁸ chlorin (Chl),^{14,19} and phthalocyanine (Pc)^{20,21} derivatives have the ability to interact with microorganisms, and their capability to generate ROS have been related with the efficiency of

microbial inactivation mediated by oxidative stress exerted at different cellular targets simultaneously,^{5,22–24} thus avoiding the development of resistance mechanisms.^{5,25} In fact, this antimicrobial approach has been successfully applied under different contexts like inactivation of pathogenic microorganisms in wastewater,^{26–28} blood disinfection,^{11,29} skin lesions,³⁰ dental infections,^{31,32} antiviral^{33,34} among others.^{1,35,36}

It is well-known that the susceptibility difference in Gram-positive *vs.* Gram-negative bacteria towards the photodynamic effect is due to the different constitution of the bacterial cell wall.^{5,23,37} The use of cationic PS as well as neutral or anionic PS accompanied by membrane disruptors (like ethylenediamine tetraacetic acid, EDTA, polymyxin B, etc) allow the close interaction between these PS and the outer membrane components (lipoproteins, lipopolysaccharides) of the Gram-negative bacteria, the most difficult to inactivate by PDI. These interactions increase the efficiency of the photodynamic process through the favourable bond of the PS to the bacteria cell wall.^{1,23,37} On the other hand, the photoinactivation of Gram-positive bacteria can be also easily achieved by neutral or anionic PSs.^{23,37} Recently, it was observed that the addition of inorganic salts, such potassium iodide (KI), can also potentiate the PDI effect of certain PSs.^{38,39} Even, some neutral or anionic PSs can photoinactivate Gram-negative bacteria when combined with KI salt.^{39–41} This extra killing effect is caused by a series of side reactions which is initiated by the reaction of $^1\text{O}_2$ with KI salt producing peroxyiodide species (HOOI_2^-), that can be degraded according two pathways depending on the PS binding degree to the microbial cell. The first pathway involves the formation of free iodine (I_2/I_3^-) and hydrogen peroxide (H_2O_2) species.^{38,41–43} The free iodine, a well-known antimicrobial agent, is able to kill microbial cells when in solution after reaching a specific threshold concentration. The amount of I_2/I_3^- is not only dependent on the amount of $^1\text{O}_2$ produced but also on the iodide anion concentration in solution.

The second pathway involves a homolytic cleavage process of HOOI_2^- producing reactive iodine radicals (I_2^\cdot) that when generated close to the target cells are much more toxic when compared with the previous mechanism. These species have a short lifetime and consequently a short diffusion distance. The occurrence of an abrupt PDI profile in the presence of KI salt means that the main contributor for that behaviour is the free iodine and a gradual photoinactivation rate means that the short-lived iodine radical is the main killing specie.⁴¹

Considering our interest in developing efficient PSs based on tetrapyrrolic macrocycles and to evaluate their photodynamic efficacy in the absence and in the presence of co-adjuvants like KI,^{38,44–46} we decided to evaluate, for the first time, how the presence of thiopyridinium or inverted methoxypyridinium units in the porphyrin core, either as free-base or as Zn(II) complexes, could affect the PS photodynamic efficacy towards a bioluminescent recombinant *E. coli* strain, used as a Gram-negative pathogenic bacteria. The establishment of this structure-activity relationship involved the previously synthesized free-base thiopyridinium Por **1b**⁴⁷ and inverted methoxypyridinium Por **2b**⁴⁸ and the corresponding new ZnPors **1c** and **2c** (Scheme 1). Additionally, the study was also extended to the neutral free-base Pors **1** and **2**^{47,48} and to their corresponding zinc(II) complexes (ZnPors **1a** and **2a**, Scheme 1), where KI was used as a potentiator of the PDI effect. The obtained photoinactivation results are discussed and compared considering the photophysical and photochemical properties of the different studied Pors.



Scheme 1

2. Experimental section

2.1. Synthesis and characterization of the photosensitizers

The Por derivatives hereafter identified by **1**, **1b**, **2**, and **2b** were synthesized according to the approach developed previously by our research group (Scheme 1).^{47,48} The corresponding ZnPor derivatives **1a**, **1c**, **2a**, and **2c** were prepared following a similar methodology as depicted also in Scheme 1. All reagents used in this work were purchased from Sigma-Aldrich and not subject to any purification process, being directly used in all reactions due to its elevated purity. The solvents were used as received or distilled and dried by standard procedures.⁴⁹ Analytical thin layer chromatography (TLC) was carried out on precoated sheets with silica gel (Merck 60, 0.2 mm thick). Column chromatography was carried out using silica gel (Merck, 35-70 mesh).

¹H and ¹⁹F NMR spectra were recorded on a Bruker AMX 300 and 400 NMR spectrometers, respectively at 300.13 and 400.13 MHz for ¹H and 282.38 and 376.46 MHz for ¹⁹F. The ¹³C NMR spectra were recorded on a Bruker AMX 400 and 500 NMR at 100.62 and 125.77 MHz, respectively. DMSO-*d*₆ was used as the deuterated solvent and tetramethylsilane (TMS) as the internal reference. The chemical shifts are expressed in δ (ppm) and the coupling constants (*J*) in Hertz (Hz). ESI-MS spectra were recorded on a Q-TOF 2 instrument (Micromass, Manchester, UK). Solutions of the samples with a concentration of 1 mg/mL were prepared dissolving the compound in CH₂Cl₂ or MeOH. Samples for ESI analysis were prepared by diluting 2 μL of the solutions with 200 μL of methanol/formic acid (0.1%). Nitrogen was used as nebulizer gas. Samples were introduced into the mass spectrometer at a flow rate of 10 $\mu\text{L}/\text{min}$, the needle voltage was set at 3000 V, with the ion source at 80 $^\circ\text{C}$ and desolvation temperature of 150 $^\circ\text{C}$. The spectra were acquired for a cone voltage of 30 V. Data acquisitions were carried out with a Micromass MassLynx 4 data system. The absorption spectra were recorded on a Shimadzu UV-2501-PC using *N,N'*-dimethylformamide (DMF) as solvent. Steady-state fluorescence spectra of PS **1**, **1a-1c**, **2** and **2a-2c** were recorded in DMF in 1 \times 1 cm quartz optical cells under PTN conditions on a computer controlled Horiba Jobin Yvon Fluoro-Max-3 spectrofluorometer. The widths of both excitation and emission slits were set at 5.0 nm. The fluorescence quantum yield (Φ_{F}) of the same Pors was calculated in DMF by comparing the area under spectrum emission of each Por with the area under the emission spectrum of 5,10,15,20-tetraphenylporphyrin (TPP) used as standard reference ($\Phi_{\text{F}} = 0.11$ in DMF).⁵⁰

2.2. Synthesis of the Zn(II) complex of the neutral and of the cationic porphyrins

2.2.1 Synthesis of 5,10,15,20-tetrakis[2,3,5,6-tetrafluoro-4-(pyridin-4-ylsulfanyl)phenyl]porphyrinato zinc(II), **1a**

5,10,15,20-Tetrakis(pentafluorophenyl)porphyrinato zinc(II) (**ZnTPPF₂₀**) (420.0 mg, 0.405 mmol), 4-mercaptopyridine (209.0 mg, 1.824 mmol) and diethylamine (188 μ L, 1.824 mmol) were left stirring overnight in 25 mL of DMF at 25 °C. Then, the reaction mixture was evaporated until dryness and purified by silica chromatography column using CH₂Cl₂/MeOH (95:5) as eluent. The obtained purple compound, after recrystallization from CH₂Cl₂/MeOH/hexane (2:1:0.5) afforded the desired pure derivative **1a** in 61% yield (350.7 mg, 0.247 mmol) being the structure confirmed through ¹H, ¹⁹F, ¹³C NMR, ESI-MS, UV-Vis and emission characterization techniques. ¹H NMR (300.13 MHz, DMSO-*d*₆): δ 7.71 (dd, *J* = 4.7, 1.5 Hz, 8H, Py-*o*-H), 8.61 (dd, *J* = 4.7, 1.5 Hz, 8H, Py-*m*-H), 9.43 (s, 8H, β -H) ppm. ¹⁹F NMR (282.37 MHz, DMSO-*d*₆): δ -137.28 (dd, *J* = 26.5, 11.3 Hz, 8F, Ar-*m*-F), -133.19 (dd, *J* = 26.5, 11.3 Hz, 8F, Ar-*o*-F) ppm. ¹³C NMR (100.6 MHz, DMSO-*d*₆): δ 103.8, 109.2, 121.1, 132.9, 144.9, 145.7 – 148.4 (CF), 149.5, 150.0 ppm. ESI-MS *m/z*: 1401.1 [M+H]⁺, 701.4 [M+2H]²⁺, 468.1 [M+3H]³⁺. UV-Vis (DMF): λ_{\max} (log ϵ): 423 (5.8), 553 (4.5) nm. Fluorescence (DMF) λ_{\max} 594, 647 nm; Fluorescence Quantum Yield (Φ_F) in DMF: Φ_F = 0.05.

2.2.2 Synthesis of 5,10,15,20-tetrakis[2,3,5,6-tetrafluoro-4-(1-methylpyridinium-4-ylsulfanyl)phenyl]porphyrinato zinc(II), **1c**

In a sealed tube, Por **1a** (76.0 mg, 0.054 mmol) and methyl iodide (3 mL, 48.1 mmol) was stirred in 10 mL of DMF for 48 h at room temperature. Afterwards, the mixture was cooled in an ice bath and the product precipitated with diethyl ether. The product was retaken in acetone, re-precipitated with CH₂Cl₂, filtered and well washed with CH₂Cl₂. The compound was dried under vacuum to yield a purple powder (75.0 mg, 38.0 μ mol, 70%). The structure was identified as **1c** by ¹H, ¹⁹F, ¹³C NMR, ESI-MS, UV-Vis and emission characterization techniques. ¹H NMR (400.13 MHz, DMSO-*d*₆): δ 4.35 (s, 12H, -NCH₃), 8.44 (d, *J* = 6.7 Hz, 8H, Py-*o*-H), 8.93 (d, *J* = 6.7 Hz, 8H, Py-*m*-H), 9.46 (s, 8H, β -H) ppm. ¹⁹F NMR (376.46 MHz, DMSO-*d*₆): δ -136.56 (dd, *J* = 26.0, 10.5 Hz, 8F, Ar-*m*-F), -132.51 (dd, *J* = 26.6, 10.5 Hz, 8F, Ar-*o*-F) ppm. ¹³C NMR (100.62 MHz, DMSO-*d*₆): δ 47.3 (NCH₃), 103.8, 107.0, 123.5, 133.0, 144.9, 145.8 – 148.4 (CF), 149.5, 156.7 ppm. ESI-MS *m/z*: 366.5 [M]⁴⁺ and 487.6 [M + 2H + e⁻]³⁺. UV-Vis (DMF): λ_{\max} (log ϵ) 421 (5.6), 553 (4.4) nm; Fluorescence (DMF) λ_{\max} 592, 645 nm; Fluorescence Quantum Yield (Φ_F) in DMF: Φ_F = 0.04.

2.2.3 Synthesis of 5,10,15,20-tetrakis[2,3,5,6-tetrafluoro-4-(1,4-dihydro-4-oxopyridin-1-yl)phenyl]porphyrinato zinc(II), **2a**

Por **2** (51.6 mg, 0.041 mmol) and zinc(II) acetate (14.8 mg, 0.081 mmol) were left stirring overnight in 5 mL of MeOH/CHCl₃ (1:1) at 60 °C. Then, the reaction mixture was evaporated until dryness, re-dissolved in MeOH, precipitated by dropwise addition of CH₂Cl₂/Hexane (1:1), filtered and washed with water to remove excess of Zn(OAc)₂. The obtained purple precipitate was isolated in 76% yield (41.4 mg, 0.031 mmol). The structure was identified as **2a** by ¹H, ¹⁹F NMR, ESI-MS, UV-Vis and emission characterization techniques. ¹H NMR (300.13 MHz, DMSO-*d*₆): δ 6.55 (d, *J* = 7.9 Hz, 8H, Py-*m*-H), 8.24 (d, *J* = 7.9 Hz, 8H, Py-*o*-H), 9.32 (s, 8H, β -H) ppm. ¹⁹F NMR (282.38 MHz, DMSO-*d*₆): δ -145.84 (dd, *J* = 26.0, 10.1 Hz, 8F, Ar-*m*-F), -134.77 (dd, *J* = 26.0, 10.1 Hz, 8F, Ar-*o*-F) ppm. ¹³C NMR (125.77 MHz, DMSO-*d*₆): δ 103.5, 118.5, 121.1, 122.3, 132.5, 141.4, 143.3 – 146.9 (CF), 149.6, 177.5 (C=O). ESI-MS *m/z*: 1337.2 [M+H]⁺, 669.4 [M+2H]²⁺, 446.8 [M+3H]³⁺. UV-Vis (DMF): λ_{\max} (log ϵ) 421 (5.6), 551 (4.2),

582 (3.3) nm. Fluorescence (DMF) λ_{\max} 592, 645 nm; Fluorescence Quantum Yield (Φ_F) in DMF: $\Phi_F = 0.05$.

2.2.4 Synthesis of 5,10,15,20-tetrakis[2,3,5,6-tetrafluoro-4-(4-methoxypyridinium-1-yl)phenyl]porphyrinato zinc(II), 2c

In a sealed tube, Por **2a** (80.0 mg, 0.060 mmol) and dimethylsulphate (300 μ L, 3.16 mmol) were dissolved in 5 mL of DMF stirring for 48 h at 80 °C. After, the mixture was cooled until room temperature, the product was precipitated with diethyl ether. The product was retaken in MeOH, re-precipitated with CH_2Cl_2 /hexane, filtered and washed with the same solvent. The compound was dried under vacuum system for 8 h at 80 °C to yield a purple powder (50.0 mg, 0.031 mmol, 53%). The structure was identified as **2c** by ^1H , ^{19}F NMR, ESI-MS, UV-Vis and emission characterization techniques. ^1H NMR (400.13 MHz, $\text{DMSO-}d_6$): δ 4.37 (s, 12H, -OCH₃), 8.20 (d, $J = 6.9$ Hz, 8H, Py-*m*-H), 9.36 (s, 8H, β -H), 9.52 (d, $J = 6.9$ Hz, 8H, Py-*o*-H) ppm. ^{19}F NMR (282.37 MHz, $\text{DMSO-}d_6$): δ -148.41 (dd, $J = 24.0, 8.5$ Hz, 8F, Ar-*m*-F), -137.60 (dd, $J = 24.0, 8.5$ Hz, 8F, Ar-*o*-F) ppm. ^{13}C NMR (100.62 MHz, $\text{DMSO-}d_6$): δ 59.3 (O-CH₃), 103.2, 114.9, 123.3, 132.5, 140.6 – 147.1 (CF), 147.9, 149.5, 173.9 ($\underline{\text{C}}$ -O-CH₃) ppm. ESI-MS m/z : 349.5 [M]⁴⁺ and 465.3 [$\text{M} + 2\text{H} + \text{e}$]³⁺. UV-Vis (DMF): λ_{\max} (log ϵ): 423 (5.6), 553 (4.4) nm. Fluorescence (DMF) λ_{\max} 597, 648 nm; Fluorescence Quantum Yield (Φ_F) in DMF: $\Phi_F = 0.04$.

2.3 Singlet oxygen generation studies

The ability of Pors **1**, **1a-1c**, **2**, **2a-2c** to generate singlet oxygen was evaluated by monitoring the photooxidation of 9,10-dimethylanthracene (9,10-DMA), a singlet oxygen quencher.^{51,52} Solutions of the Pors derivatives and **TPP** in DMF ($\text{Abs}_{418} \sim 0.20$) were aerobic irradiated in quartz cuvettes with monochromatic light ($\lambda = 420$ nm) in the presence of 9,10-DMA (~ 50 μM). A solution of **TPP** in DMF was used as reference ($\Phi_\Delta = 0.65$).^{50,53} The kinetics of 9,10-DMA photooxidation was studied by following the decrease in its absorbance at 378 nm and the result registered in a first-order plot for the photooxidation of 9,10-DMA photosensitized by Pors **1**, **1a-1c**, **2**, **2a-2c** and **TPP** in DMF. The kinetics of 9,10-DMA photooxidation in the absence of any compound was also studied and no significant photodegradation was observed under irradiation at 418 nm in DMF. The results are expressed as mean and standard deviation obtained from three independent experiments with two replicates.

2.4 Photodynamic inactivation studies

2.4.1 Photodynamic inactivation studies and bioluminescence monitoring

Bioluminescent *E. coli* culture was grown overnight in ≈ 30 mL of Tryptic Soy Broth (TSB) and diluted in PBS (pH = 7.49) to a final concentration of $\sim 10^7$ CFU.mL⁻¹ (corresponding nearly to 10^7 RLU). The *E. coli* suspension was equally distributed in a sterilized 6-well cell culture plate. The bioluminescent *E. coli* suspension was exposed to PSs **1**, **1a**, **2**, **2a** at 5.0 and 1.0 μM and **1b**, **1c**, **2b**, **2c** at 5.0, 2.5 and 1.0 μM that were achieved with the addition of appropriate volumes of each Por stock solution. For PS **1**, **1a**, **2** and **2a** the combined effect of each Por with the potentiator agent KI salt at 100 mM was also evaluated. The samples and controls were protected from light with aluminium foil and were maintained in the dark for 10 min to promote the PS binding to bioluminescent *E. coli* cells. Light control (LC) comprising bacterial suspension exposed to the same light condition as the samples, light control with KI (LC+KI) comprising bacterial suspension with 100 mM of KI exposed to the same light condition as the samples and dark controls (DC) comprising bacterial suspension incubated with the PS at 5.0

μM and protected from light were also evaluated. After the incubation period, samples and controls were exposed to the white light irradiation under stirring (400 rpm); the room was maintained cooled in order to keep the samples at constant temperature (25 °C). Aliquots of 1.0 mL of samples and controls were collected at different times of light exposure and the bioluminescence signal was measured in the luminometer (TD-20/20 Luminometer, Turner Designs, Inc., Madison, WI, United States). The assays were finished whenever the detection limit of the luminometer was achieved (*ca.* 2.3 log).

Simultaneously, aliquots of treated and control samples were collected at time 0 and 60 min or when the detection limit of the luminometer was achieved, serially diluted and pour-plated in duplicate in Tryptic Soy Agar (TSA) medium. The petri plates were incubated for 24 h at 37 °C and the concentration of viable cells was determined by counting the CFU on the most appropriate dilution. Three independent experiments with three replicates were performed and the results averaged.

2.4.2 Photosensitizer binding studies

Bioluminescent *E. coli* suspension adjusted for $\approx 10^7$ CFU mL⁻¹ in PBS was incubated for 10 min in the dark at 25 °C alone or in the presence of each PS (**1**, **1a-1c** and **2**, **2a-2c**) at the same concentrations used in the photoinactivation studies (1.0, 2.5 and 5 μM for cationic species – **1b**, **1c**, **2b**, **2c** – and 1.0 and 5.0 μM with and without KI (100 mM) for neutral species – **1**, **1a**, **2**, **2a**). The unbound PS was removed from the suspension by centrifugation at 9500 g for 5 min (Gyrozen 1730R, Korea). The pellets were washed with PBS (3x) and then centrifugated at the same conditions. The washed pellets were then resuspended in 80 μL of DMSO and vigorously agitated in the vortex, to promote the PS dissolution. The content was transferred into a black 96-well-plate and the fluorescence of the cells bounded PS was measured using a Synergy HT Pro microplate reader (BioTek Instruments, EUA) with GEN5 software with excitation set at 550 nm and emission set at 590 nm. The measured fluorescence intensity allowed the determination of the corresponding concentration by interpolation with a calibration plot made with established concentrations of each PS.

Simultaneously, aliquots of 100 μL of the samples and control after incubation time were collected, serially diluted and plated in TSA for the determination of the concentration of viable cells (CFU.mL⁻¹). The results were shown in nmol PS/log(CFU). Three independent assays were performed, and the results averaged.

3. Results and discussion

3.1 Synthesis, photophysical and photochemical characterization of the porphyrin derivatives

The neutral (**1** and **2**) and cationic (**1b** and **2b**) free-base Pors were prepared according to Gomes *et al.*⁵⁴ and Costa *et al.*⁴⁷ The zinc(II) complexes **1a** and **2a** were prepared using different sequential approaches: i) in case of Por **1a** (61%), the nucleophilic substitution reaction with 4-mercaptopyridine was performed after metalation of the starting template 5,10,15,20-tetrakis(pentafluorophenyl)porphyrin (**H₂TPPF₂₀**) with zinc acetate to obtain the **ZnTPPF₂₀**; and ii) in case of Por **2a** (74%), the reaction of **H₂TPPF₂₀** with the 4-hydroxypyridine affording the free-base **2** preceded the metalation step with zinc acetate. These metalation reactions were easily followed by UV-Vis, being possible to observe the disappearance of one of the Q bands of the corresponding free-base Por, due to the symmetry increase, characteristic of metalloporphyrins (Figure 2). The ZnPors **1c** and **2c** (Scheme 1) were prepared through cationization of ZnPors **1a** and **2a** with methyl iodide and dimethylsulphate, respectively. Both

cationic ZnPors (**1c** and **2c**) were isolated in moderate yields (70 and 53%, respectively). The structures of all Pors were confirmed by NMR spectroscopy (Figs. SI 1-12), ESI-MS spectrometry (Figs. SI 13-16), UV-Vis absorption and emission spectroscopy (Figure 1).

The positive mode ESI-MS spectra of the ZnPors **1a** (m/z 1401.1 $[M+H]^+$, 701.4 $[M+2H]^{2+}$, 468.1 $[M+3H]^{3+}$, Fig. SI 13) and **2a** (m/z 1337.2 $[M+H]^+$, 669.4 $[M+2H]^{2+}$, 446.8 $[M+3H]^{3+}$, Fig. SI 15) were acquired CH_3OH /formic acid and show, besides the formation of the expected mono-charged ion $[M+H]^+$ the formation of multi-charged ions due to the di- and tri-protonation of the basic sites present in the porphyrin core.⁵⁵ In case of the tetracationic derivatives ZnPors **1c** and **2c** were observed the expected peaks at m/z 366.5 and 487.6 (Fig. SI 14) and m/z 349.5 and 465.3 (Fig. SI 16) respectively corresponding to the expected $[M]^{4+}$ and also the resulting reduction $[M + 2H + e]^{3+}$ species.

The absorption and emission spectra of Pors **1**, **1a-1c** and Pors **2**, **2a-2c** were recorded in DMF solutions at 298 K (Figure 1). All the main photophysical features such as Soret and Q band wavelengths, molar extinction coefficients (ϵ), fluorescence emission wavelengths (λ_{emiss}), Stokes shift and fluorescence quantum yields (Φ_F) are summarised in Table 1.

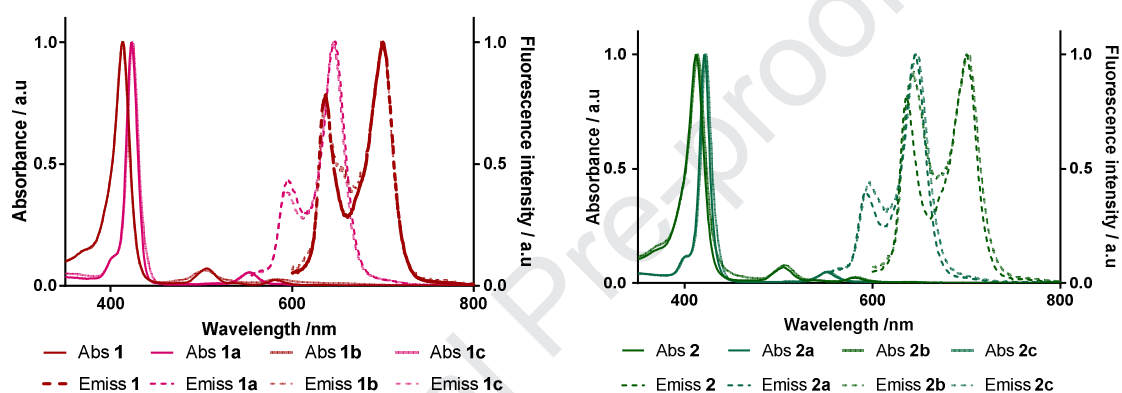


Figure 1. Normalized absorption (solid lines) and emission (dashed lines) spectra of Pors **1**, **1a-1c** and Pors **2**, **2a-2c** in DMF at 298 K.

The UV-Vis absorption spectra of Pors **1**, **1b** and Pors **2**, **2b** in DMF solutions exhibit a typical free-base Por features with a strong Soret band at *ca.* 400 nm and three Q bands between 450 and 700 nm (Figure 1, solid lines).

The steady-state fluorescence spectra of Pors **1**, **1a-1c** and Pors **2**, **2a-2c** were also achieved in DMF (Figure 1, dashed lines) and exhibit a two strong emission between 600 and 750 nm. The fluorescence quantum yields (Φ_F) of the free-base Pors **1**, **1b** and Pors **2**, **2b** and of their ZnPors **1a**, **1c** and ZnPors **2a**, **2c** are presented in Table 1, where it's showed that they are lower than the standard reference Por **TPP** in DMF ($\Phi_F = 0.11$).⁵⁰ It is worth to refer that the emission and the fluorescence quantum yield were affected by the metalation as expected.⁵⁶

Table 1. Photophysical properties of Pors **1**, **1a-1c** and Pors **2**, **2a-2c** in DMF.

Compound	Soret (nm)	log ϵ	Q bands (nm)	log ϵ	λ_{emiss} (nm)	Φ_F^a	$\Phi_A \pm 0.05^a$
1	413	5.6	506	4.4	637 700	0.06	0.87
			581	3.9			
			634	3.1			
1a	423	5.8	553	4.5	594 647	0.05	0.66
1b	413	5.6	505	4.3	636 701	0.02	0.47
			583	4.0			
1c	421	5.6	553	4.4	592 645	0.04	0.56

2	412	5.5	505	4.3	637 701	0.08	0.91
			580	3.9			
			646	3.1			
2a	421	5.6	551	4.2	592 645	0.05	0.56
			582	3.3			
2b	413	5.5	507	4.4	642 704	0.03	0.35
			583	3.9			
2c	423	5.6	553	4.4	597 648	0.04	0.28

^aUsing **TPP** as reference in DMF.

The generation of $^1\text{O}_2$ (Fig. SI 17) was assessed considering that it is, in general, the major ROS produced upon irradiation by this type of compounds and one of the main responsible specie for cell damage and further cell death. Thus, the production of $^1\text{O}_2$ by each Por was assessed indirectly by the absorption decay of 9,10-DMA solution irradiated in the presence of each PS (**1**, **1a-1c** and **2**, **2a-2c**) having as comparison the good $^1\text{O}_2$ generator **TPP** ($\Phi_{\Delta} = 0.65$ in DMF).⁵³ According to the obtained results summarized in Table 1, all derivatives are able to generate singlet oxygen species upon light irradiation and the free-base Pors **1** and **2** clearly generate more singlet oxygen than the ZnPors **1a** and **2a** under same irradiation conditions. As far as the cationic porphyrins are concerned the ZnPor **1c** shows a slight better performance to generate $^1\text{O}_2$ than the free-base **1b** (0.56 *versus* 0.47) while the opposite is observed for Pors **2b** and **2c** (0.35 *versus* 0.28).

It is also important to mention that UV-Vis spectrum of PS solution during its irradiation in the presence of 100 mM of KI, showed a new band formation between 340 and 355 nm due to the appearance of iodine specie (Fig. SI 20).^{38,57} Here, it is possible to say that during the photodynamic process, there will be iodine present which in case of reaching a specific threshold, it is possible to kill additionally bacteria. In order to confirm the presence of iodine specie in the solution it was performed the simple test with the amylose of the starch, which produces a purple color in the presence of iodine. The results of this assay are present in Figure 2 for the neutral Pors (**1**, **1a**, **2** and **2a**) where it is possible to see the purple color in the samples that were used in the photostability assay after the addition of three drops of a starch solution.

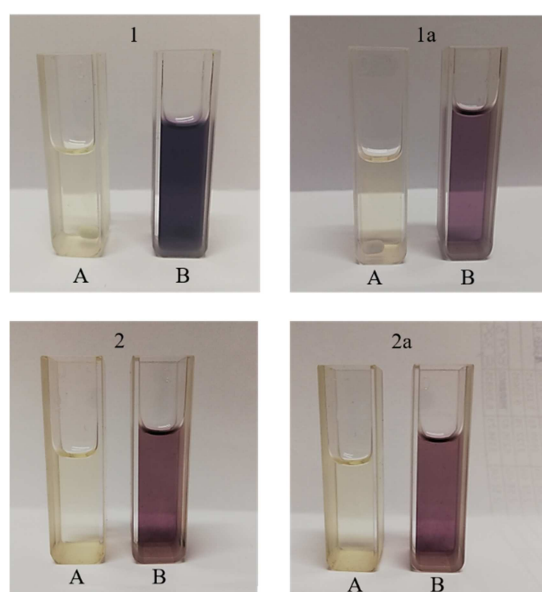


Figure 2. Starch test to assess if there was iodine present in the irradiated solution in the presence of 100 mM of KI. A – PS solution added with 100 mM of KI and three drops of starch

before irradiation and B – PS solution added with 100 mM of KI and three drops of starch after irradiation.

It is noteworthy that in case of the irradiated samples (B), there was the presence of free iodine derived from the reaction of water with peroxyiodide which, in turn, came from the reaction with singlet oxygen and potassium iodide.

The photophysical and photochemical properties described above for all studied Pors, make them suitable to be used as potential PSs against Gram-negative *E. coli* bacterium. In fact, the formation of iodine species can help to elucidate the mechanism of the photodynamic process.

3.4 Photodynamic inactivation of bioluminescent *Escherichia coli*

3.4.1. Photodynamic effect of cationic PS 1b, 1c, 2b and 2c

The free-base thiopyridinium Por **1b** already proved to be efficient in the photoinactivation of *Penicillium chrysogenum conidia*,⁵⁴ *S. aureus* and *P. aeruginosa*.⁴⁷ Having in mind these results, it was considered relevant to extend these PDI studies against the bioluminescent *E. coli*, and at the same time to see how the distribution of the positives charges in the macrocycle and the presence of Zn in its inner core affect the photodynamic action. So, in this section the PDI results obtained with the cationic free-base porphyrins **1b** and **2b** and with their Zn(II) complexes **1c** and **2c** are discussed.

The photodynamic efficiency of the cationic PSs **1b**, **1c**, **2b** and **2c** against the recombinant bioluminescent *E. coli*, was evaluated at concentrations 5.0, 2.5 and 1.0 μM under photosynthetically active radiation (PAR) white light at an irradiance of 25 $\text{mW}\cdot\text{cm}^{-2}$. The results obtained are summarized in Figure 3 and had shown that the inactivation profile of bioluminescent *E. coli* with cationic Por derivatives **1b**, **1c**, **2b** and **2c** is dependent on the tested concentration. Also, in these cases, LC and DCs did not promote a decrease on the bioluminescence *E. coli* signal, showing that the viability of this recombinant bioluminescent bacterium was not affected by irradiation and by the presence of PS.

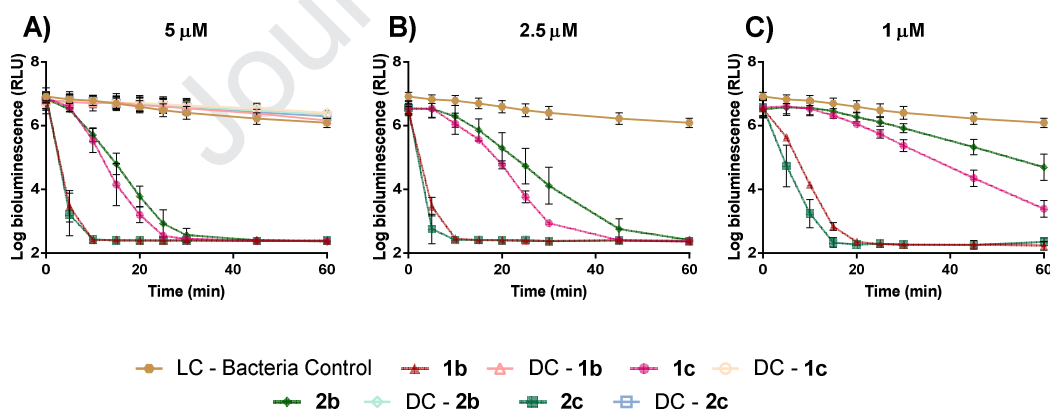


Figure 3. Bioluminescence monitoring of bioluminescent *E. coli* treated with cationic PSs **1b**, **1c**, **2b** and **2c** at 5.0, 2.5 and 1.0 μM after 60 min of irradiation with white light at an irradiance of 25 $\text{mW}\cdot\text{cm}^{-2}$. The values are expressed as the means of three independent experiments with replicates; error bars indicate the standard deviation; DC - dark control; LC - light control.

As expected for Gram-negative bacteria, the cationic Por derivatives had promoted higher decrease in the bioluminescence signal of *E. coli* when compared with the neutral derivatives (when were tested alone). The most effective PSs seems to be derivatives **2c** and **1b**, since, at the lowest concentration tested (1.0 μM), the decrease of the bioluminescent signal of *E. coli* promoted by these compounds achieved the detection limit (decreases of 4.1 \log_{10} , ANOVA, *p*

< 0.001) after 20 min of irradiation (Figure 3C). When these compounds were evaluated at 2.5 and 5.0 μM (Figure 3B and 3A, respectively), the detection limit of the methodology was achieved sooner, after 10 min of the PDI protocol. Cationic Pors **1c** and **2b** at 1.0 μM (Figure 3C) were also capable to photoinactivate *E. coli*, promoting a decrease of 2.7 \log_{10} and 1.4 \log_{10} (ANOVA, $p < 0.0001$), after 60 min of irradiation. At 2.5 μM Por **1c** (Figure 3B) had promoted a decrease of the bioluminescent signal of *E. coli* of 2.8 \log_{10} (ANOVA, $p < 0.0001$) after 30 min of the PDI protocol, achieving the detection limit after 45 min of PDI protocol. At the same concentration, Por **2b** had affected the viability of the recombinant bacterium causing a decrease of 3.5 \log_{10} (ANOVA, $p < 0.0001$) in the bioluminescence after 45 min of irradiation achieving the detection limit of the methodology after 15 min. At the higher concentration (5.0 μM , Figure 3A) these PSs presented similar photodynamic profiles, causing a significant decrease in the bioluminescence of *E. coli* till the detection limit of the methodology (decreases of 3.7 \log_{10} , ANOVA, $p < 0.001$) after 30 min of irradiation.

In order to correlate the bioluminescence reduction of *E. coli* with the reduction of $\text{CFU}\cdot\text{mL}^{-1}$ at the lower tested concentration (1.0 μM), the above study was accompanied by the pour plate methodology. Thus, aliquots of the samples and controls were collected at times 0 and 60 min of the PDI assay, serially diluted in PBS and plated in triplicate in TSA. The results are presented in Figure 4.

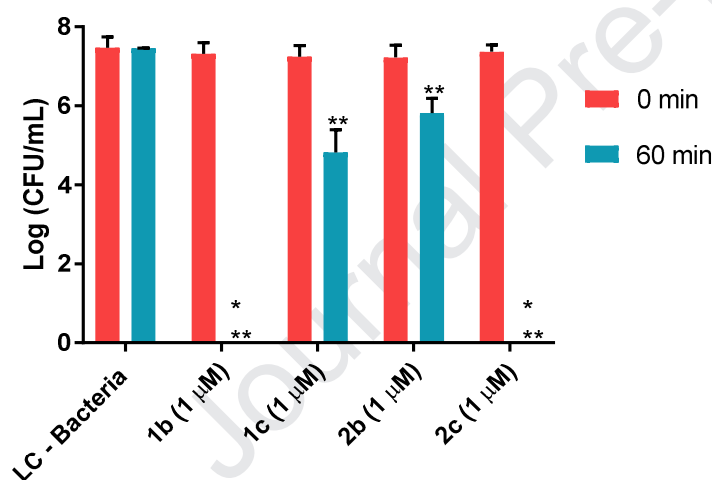


Figure 4. Photodynamic inactivation of *E. coli* treated with cationic PSs **1b**, **1c**, **2b** and **2c** at 1.0 μM after 60 min of irradiation with white light at an irradiance of $25 \text{ mW}\cdot\text{cm}^{-2}$. The values are expressed as the means of two independent experiments; error bars indicate the standard deviation; * there was no colony present; ** ($p < 0.0001$) significantly different from time 0.

These results confirm that the PSs **1b** and **2c** were the most efficient PSs, causing a viability decrease of 7.3 \log_{10} (ANOVA, $p < 0.0001$) in the viability of *E. coli* after 60 min of irradiation ($90 \text{ J}\cdot\text{cm}^{-2}$). Additionally, the ZnPor **1c** and Por **2b** promoted lowest decrease in photoinactivation of *E. coli* of 2.6 and 1.6 \log_{10} (ANOVA, $p < 0.0001$), respectively. These results also confirm that the irradiation (LC) does not affect the viability of *E. coli*.

It is important to highlight that the results regarding the free-base PSs **1b** and **2b** showed that the thiopyridinium Por **1b** could cause a higher decrease in the bioluminescence signal of *E. coli* than the methoxypyridinium Por **2b**, meaning that the inserted charged units can directly influence the photodynamic activity. The results also showed that the insertion of Zn(II) in the nucleus of the cationic Pors **1b** and **2b** seems to significantly improve the photoinactivation activity of Por **2b**, but the same was not verified for Por **1b** which as free-base have a better

activity than ZnPor **1c**. This could be related with their spatial geometry which could directly influence their uptake in the bioluminescent *E. coli*. To understand this fact, PSs binding studies were also performed for compounds **1b**, **1c**, **2b** and **2c** for all tested concentrations. The amount of cationic PSs (**1b**, **1c**, **2b** and **2c**) bound to the bioluminescent *E. coli* cells after 10 min of incubation in the dark is presented in Figure 5.

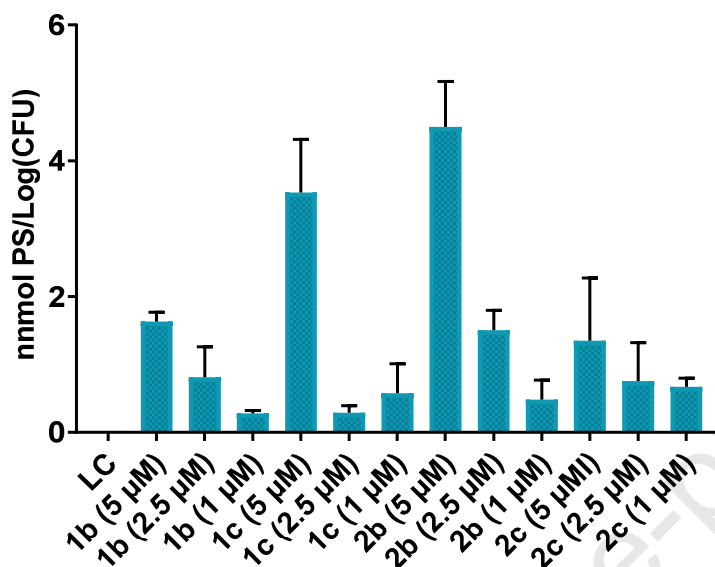


Figure 5. Amount of cationic PSs (**1b**, **1c**, **2b** and **2c**) delivered at concentration of 5.0, 2.5 and 1.0 μM bound to *E. coli* cells after 10 min of incubation in the dark at 25 °C. Values correspond to the average of three independent experiments. Error bars represent the standard deviation.

The binding PS studies showed that the adsorption (uptake) of each PS by bacterial cells is proportional to the PS concentration tested. At 5.0 μM , PSs **1c** and **2b** presented the highest adsorption values with 3.5 and 4.5 $\text{nmol} \cdot \text{Log}(\text{CFU})^{-1}$, respectively. For the same concentration, PSs **1b** and **2c** presented lower adsorption values [1.6 and 1.4 $\text{nmol} \cdot \text{Log}(\text{CFU})^{-1}$, respectively]. These results suggest that the most effective PSs in the inactivation of *E. coli* (Por **1b** and **2c**) have modest adsorption values to the PS uptake by *E. coli* cells. Once again, we cannot neglect all factors that can contribute to the efficiency of a PS during the photodynamic process. For example, although Por **1c** presented one of the highest adsorption values and $^1\text{O}_2$ quantum yield, the PDI efficiency toward *E. coli* fell short of the results achieved for Por **1b** and **2c**.

Comparing the results with the ones achieved with the structural analogue 5,10,15,20-tetrakis(1-methylpyridinium-4-yl)porphyrin tetra-iodide (**Tetra-Py(+)-Me**), it is possible to observe that this compound at 5.0 μM when acting alone with 10 times less irradiance had promoted a total inactivation of bioluminescent *E. coli* after 70 min of irradiation (10.5 J/cm^2).³⁸ In the case of metal free tetra-substituted porphyrins **1b** and **2b** the total inactivation of bioluminescent *E. coli* was achieved after 5 min (7.5 J/cm^2) and 30 min of irradiation (45 J/cm^2), respectively. These results suggest that PS **1b** is more efficient than the widely studied **Tetra-Py(+)-Me**, most probably due to the higher rotational mobility of the methylpyridinium-4-sulphonyl subunit in porphyrin **1b**, allowing a better target adhesion to the bacterium. On the contrary, PS **2b** showed to be less efficient than **Tetra-Py(+)-Me**, which can be justified by the less exposed localization of the positive charges in the macrocycle. In the case of **Tetra-Py(+)-Me** the charges are localized at the periphery of the macrocycle, favouring the adhesion to *E. coli*, enhancing its photodynamic efficiency.

Nevertheless, other factors such as PS distribution and localization cannot be neglected when trying to understand the relationship between the structural and photophysical properties with their PDI efficiency.

3.4.2. Photodynamic effect of neutral PSs 1, 1a, 2 and 2a

The high efficacy of the neutral porphyrins **1**, **1a**, **2** and **2a** to generate $^1\text{O}_2$ prompt us to evaluate their photodynamic action against the recombinant bioluminescent *E. coli* in the absence in the presence of KI. The effect of these neutral PSs was evaluated at 5.0 and 1.0 μM under the same irradiations conditions used for the cationic PSs mentioned above (Figure 6). The assays with KI were performed using this salt at 100 mM and the PSs also at 5.0 and 1.0 μM . The KI concentration was selected considering the results obtained in previous studies and knowing that higher concentrations can limit the protocol to clinical area due to the osmotic stress.^{38,44}

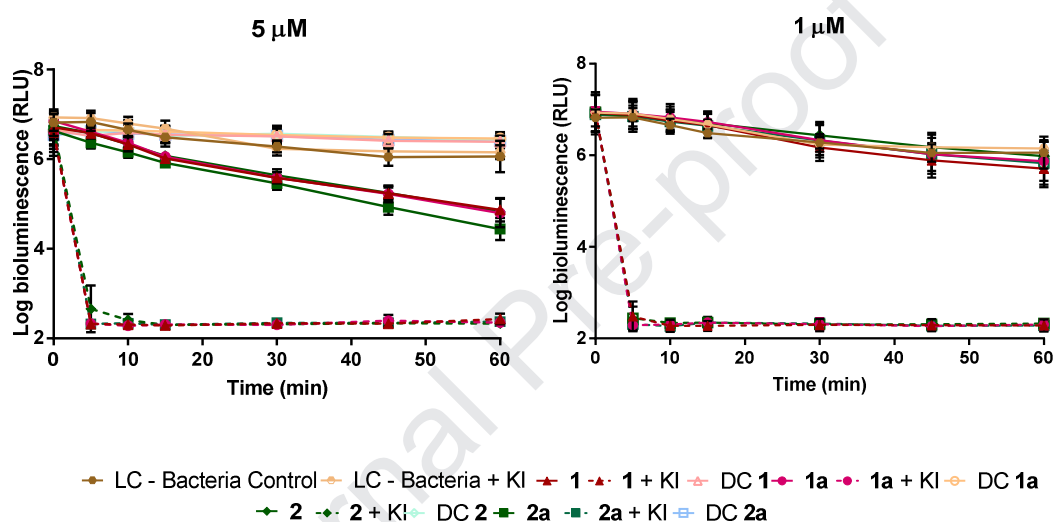


Figure 6. Bioluminescence monitoring of *E. coli* treated with PSs **1**, **1a**, **2** and **2a** at 5.0 (left) and 1.0 μM (right) at different periods of time, under white light irradiation of $25.0 \text{ mW}\cdot\text{cm}^{-2}$. The values are expressed as the means of three independent experiments; error bars indicate the standard deviation; DC - dark control; LC - light control.

In the cases of the LCs (bacteria and bacteria with KI) and DC (bacteria with PS in the dark) no decrease in *E. coli* bioluminescent signal was detected. These results indicate that the viability of this recombinant bioluminescent bacterium was not affected by irradiation, by presence of the KI salt or by the PS in the dark at the highest tested concentration.

The obtained results for the neutral PSs **1**, **1a**, **2**, **2a** at 5.0 and 1.0 μM (Figure 6

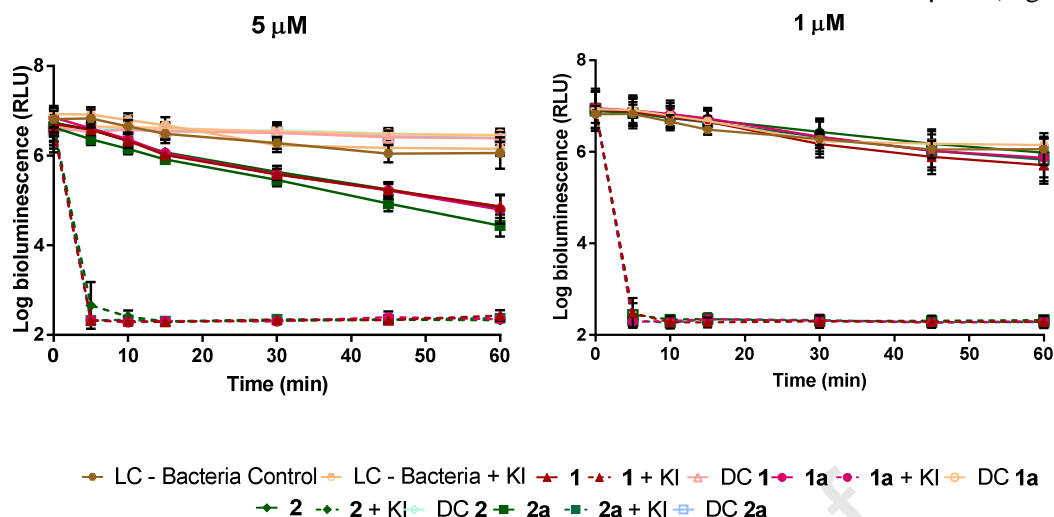


Figure 6) demonstrated that their efficacy is strongly improved by the presence of KI. In the case of results achieved after photodynamic treatment only with the PS at a concentration of 1.0 μM , no significant reductions on the bioluminescence of *E. coli* was attained. However, when these PSs **1**, **1a**, **2**, **2a** at concentrations of 1.0 μM were combined with KI at 100 mM it was observed a decrease of the bioluminescent signal till de limit of detection of the methodology [reduction $> 4.3 \log_{10}$ (ANOVA, $p < 0.0001$)] after 5 min of irradiation. When these PS were tested at 5.0 μM alone, PS **1a** and **2a** had promoted equal photoinactivation rates with decreases of the bioluminescent signal of $1.3 \log_{10}$ (ANOVA, $p < 0.0001$). PS **1** at 5.0 μM caused a decrease of the bioluminescent signal of the *E. coli* of $1.2 \log_{10}$ (ANOVA, $p < 0.0001$) and PS **2** was the less efficient PS, causing a decrease of $0.9 \log_{10}$ (ANOVA, $p < 0.0001$). As in the previously case, the combination of these PSs at 5.0 μM with KI had promoted a decrease of the bioluminescent signal till de limit of detection of the methodology [reduction of $4.3 \log_{10}$ (ANOVA, $p < 0.0001$)] after 5 min of irradiation.

These results show that all these PSs, although being neutral, when combined with KI are capable to photoinactivate a Gram-negative bacterium. A similar effect, in this case using the anionic 5,10,15,20-tetrakis(4-sulfonatophenyl)porphyrin dihydrochloride (**TPPS₄**), was also reported by Hamblin, where the combination of this anionic PS with KI had promoted the efficient photoinactivation of *E. coli*.⁴⁰ Also, Hamblin *et al.* had shown that the addition of KI (100 mM) to xanthene Rose Bengal (a non-efficient PS to photoinactivate Gram-negative bacteria when used alone), potentiated its effect in the photoinactivation of the Gram-negative *E. coli* and *P. aeruginosa*.⁵⁸ More recently, an efficient combination of the Rose Bengal and Eosin with KI was reported in the photoinactivation *S. Typhimurium*, a Gram-negative bacterium.⁵⁹ It was also demonstrated, for the first time, that the photoinactivation of *S. Typhimurium* by both xanthenes with KI did not induce the development of resistance.

It is important to highlight that according with the test of the amylose in starch (Figure 2) and the killing curve of bioluminescent *E. coli* (Figure 6) 6

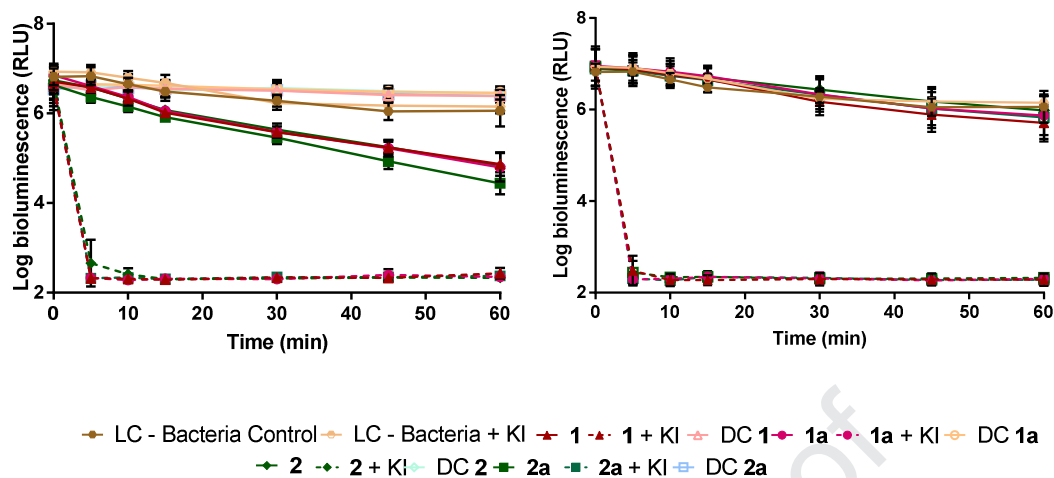


Figure 6), it is possible to observe that the produced free iodine specie reached a sufficient threshold that could photoinactivate to the detection limit of the method *E. coli* after 5 min of irradiation. Due to the abrupt decrease in the *E. coli* survival (Figure 4) it is possible to infer that the mechanism of action of the combination of PS **1**, **1a**, **2**, **2a** and KI is probably related to the preferential decomposition of the peroxyiodide into free iodine (I_2/I_3^-).^{38,41,42}

In order to correlate the bioluminescence reduction of *E. coli* with the reduction of CFU mL⁻¹ with the smallest concentration of PS (1.0 μM), the previous study was accomplished with the pour plate methodology. So, aliquots of the samples and controls were collected at times 0 and 60 min of the PDI assay, serially diluted in PBS and plated in triplicate in TSA. The results are presented in Figure 7.

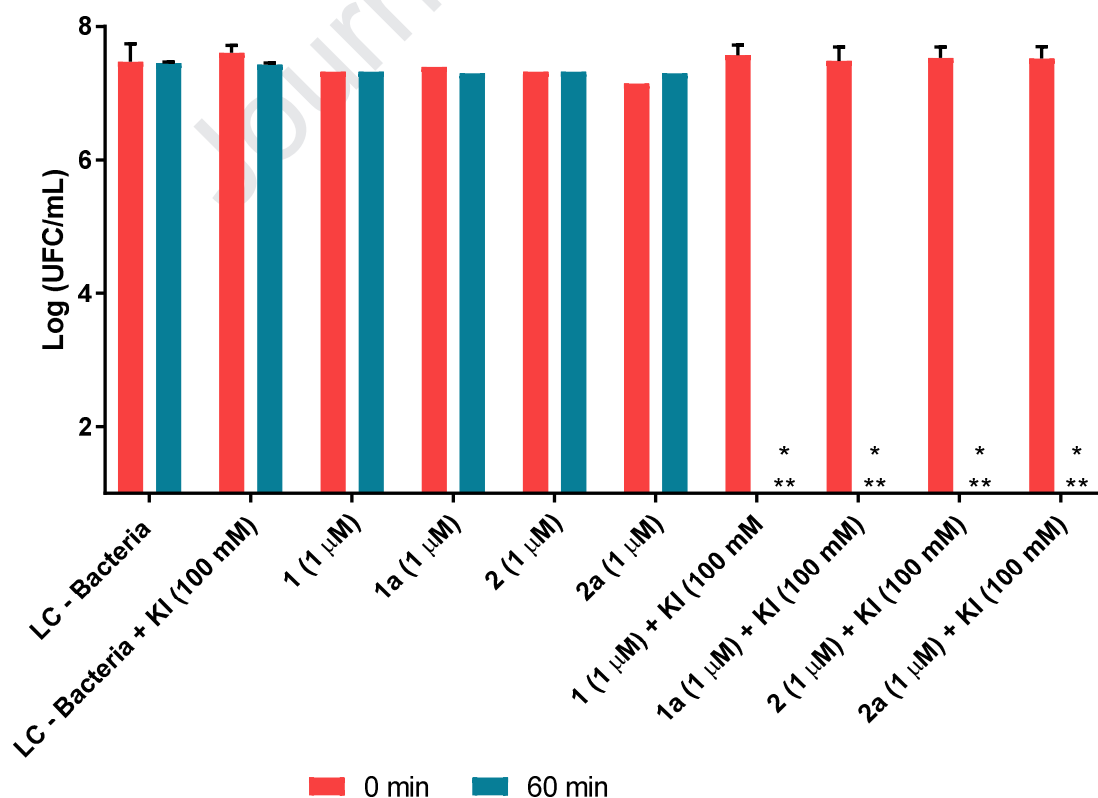


Figure 7. Photodynamic inactivation of bioluminescent *E. coli* treated with PSs **1**, **1a**, **2** and **2a**

at 1.0 μM with and without KI (100 mM) after 60 min of irradiation with white light at an irradiance of 25 $\text{mW}\cdot\text{cm}^{-2}$. The values are expressed as the means of two independent experiments; error bars indicate the standard deviation; * there was no colony present; ** ($p < 0.0001$) significantly different from time 0.

The results showed that, as previously mentioned, KI potentiated the PDI effect of Pors **1**, **1a**, **2** and **2a** when combined with KI at 100 mM. These combinations caused a bacterial viability decreasing of 7.5 log (ANOVA, $p < 0.0001$) of *E. coli* after 60 min of light irradiation (25 $\text{mW}\cdot\text{cm}^{-2}$). These results also confirm that the irradiation (LC - bacteria) and KI (LC - bacteria with KI) does not affect the viability of the bioluminescent *E. coli*. It is also evident that when these PSs act alone, no effect on the viability of *E. coli* was observed.

In order to explain the results of the PDI assays and access the influence of KI in adsorption of PS to *E. coli*, PS binding studies were performed. The amount of neutral PSs (**1**, **1a**, **2** and **2a**) bound to *E. coli* cells after 10 min of incubation in the dark at 25 °C is summarized in Figure 8.

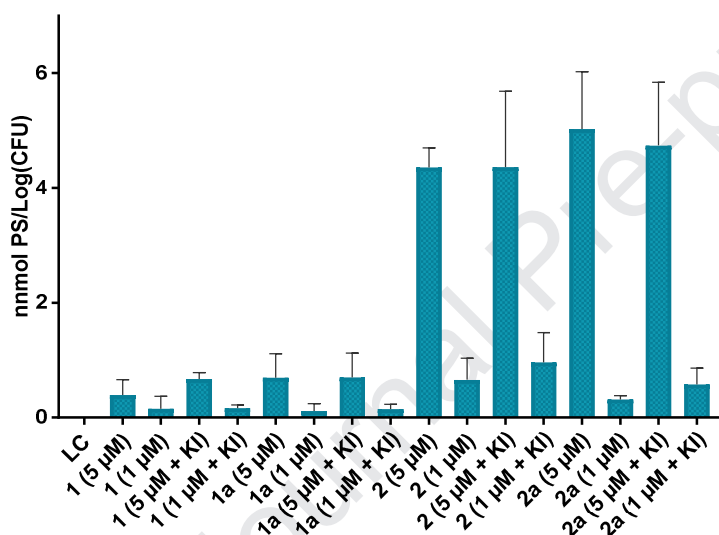


Figure 8. Amount of neutral PSs (**1**, **1a**, **2** and **2a**) delivered at the concentration of 5.0 and 1.0 μM in the absence or presence of KI at 100 mM bound to *E. coli* cells after 10 min of incubation in the dark at 25 °C. Values correspond to the average of three independent experiments. Error bars represent the standard deviation.

PSs **2a** and **2** at 5 μM , showed the highest adsorption to *E. coli* cells with an average value of 5.0 and 4.4 $\text{nmol}\cdot\text{Log}(\text{CFU})^{-1}$, respectively. PSs **1** and **1a** presented the lowest adsorption having an average of 0.4 and 0.7 $\text{nmol}\cdot\text{Log}(\text{CFU})^{-1}$, respectively. It is also possible to observe that neither KI nor the insertion of Zn(II) seems to influence the adsorption of Pors **1**, **1a**, **2** and **2a** by the bioluminescent *E. coli*. On the other hand, the different substituents units in the Por skeleton (thiopyridyl or pyridinone) promoted different results in the binding studies: the pyridinone Por **2** and ZnPor **2a** have better adsorption (4 times higher) when compared with the corresponded thiopyridyl Por **1** and ZnPor **1a**. This aspect can be due to the PS localization in the bacterial cell which will be also responsible for the different photodynamic behaviour profile.

The adsorption results can justify, in one hand, the higher PDI effect of Por **2a** (5.0 μM) in the absence of KI. However, this cannot support the equal activity of PS of **1a** which revealed one of the lowest adsorption values. It is well documented that the photodynamic inactivation

efficiency of PSs is dependent not only by the PS affinity to the bacterial cell but also by the singlet oxygen generation capacity and the amphiphilic character of the molecule.⁶⁰ In this case, PSs **1a** have higher capability to generate $^1\text{O}_2$ when compared to **2a**, which may explain the similarity of the photodynamic efficiencies of these PSs. The same concept could explain the results achieved with PS **1**: this compound has one the lowest value of adsorption to *E. coli*, however it was not the less efficient in the photoinactivation of *E. coli*. Looking to the quantum yield of $^1\text{O}_2$ generation it is possible to observe that this value is similar to compound **2a**, which may also explain the photodynamic efficiency. PS **2**, besides the high affinity to *E. coli* cell and the higher yield $^1\text{O}_2$, was the less efficient PS in the photoinactivation of this bacterium. To understand this behavior, we cannot neglect other factors that can also contribute to the efficiency of these PSs, such as aggregation behavior and photostability. In fact, PS **2** revealed to be the less stable compound when in solution, having higher rates of photodecomposition when irradiated in the PDI conditions and higher aggregation behavior (when maintained in solution in dark). These two factors can justify the poor ability to photoinactivate *E. coli*. The results achieved in this study are really promising when compared with the ones previously reported for the neutral analogue 5,10,15,20-tetra(4-pyridyl)porphyrin (Tetra-Py) in the photoinactivation of bioluminescent *E. coli*;³⁸ this PS alone or combined with KI was not able to photoinactivate this bacterium, even after 240 min of irradiation (36 J/cm^2). However, the neutral PSs **1** and **2** were able to inactivate *E. coli*, showing higher photoinactivation rates, even in the absence of KI. This fact could be also due to the higher aggregation behavior observed for Tetra-Py in aqueous media, limiting its action as a PS.

4. Conclusion

The ZnPors **1c** and **2c** were prepared and structurally characterized by NMR, UV-Vis absorption, emission spectroscopy and mass spectrometry. The photophysical and photochemical studies showed that all the synthesized Pors (**1**, **1a-1c** and **2**, **2a-2c**) were able to generate singlet oxygen species and presented moderated photostability under white light irradiation.

From the PDI studies it was found that even the neutral Pors **1**, **1a**, **2** and **2a**, at 5.0 and 1.0 μM when combined with KI were capable to photoinactivate efficiently Gram-negative bacterium bioluminescent *E. coli*. The starch assays led us to infer that the free iodine produced reached an enough threshold that could photoinactivate completely *E. coli* after 5 min of white light irradiation.

Cationic PSs **1b**, **1c**, **2b** and **2c** were also effective as PSs in the photoinactivation of the Gram-negative bacterium. At concentration of 5.0 μM , all these PSs promoted a decrease in the viability of *E. coli* till the detection limit of the methodology. However, at lower concentrations, 1 μM , only PSs **1b** and **2c** were capable to promote a decrease in *E. coli* bioluminescent signal till the method detection limit, after 20 and 15 min of treatment, respectively.

The binding studies of all neutral and cationic Por showed that the PDI efficiency of each PS, are related not only to the PSs uptake by *E. coli* cells, but also to their capability to generate $^1\text{O}_2$, photostability and aggregation behavior, charge distribution and amphiphilicity.

Acknowledgements

Thanks are due to the University of Aveiro and FCT/MCTES for the financial support to LAQV-REQUIMTE (UIDB/50006/2020), QOPNA (FCT UID/QUI/00062/2019), CESAM (UIDB/50017/2020 + UIDP/50017/2020) and Centro de Química Estrutural

(UIDB/00100/2020) research units, and to the FCT projects (P2020-PTDC/QUI-QOR/31770/2017 and P2020-PTDC/QEQ-SUP/5355/2014), through national funds (PIDDAC) and where applicable co-financed by the FEDER-Operational Thematic Program for Competitiveness and Internationalization-COMPETE 2020, within the PT2020 Partnership Agreement. We acknowledge the financial support from the RNEM (LISBOA-01-0145-FEDER-402-022125) and Node IST-Campus Alameda for facilities. Thanks, are also due to the Portuguese NMR and Mass Networks. J. Calmeiro and S. Gamelas thanks FCT for their research fellow and PhD scholarship (BI/UI51/7965/2017 and SFRH/BD/143549/2019, respectively).

5. References

- (1) Hamblin, M. R. Antimicrobial Photodynamic Inactivation: A Bright New Technique to Kill Resistant Microbes. *Curr. Opin. Microbiol.* **2016**, *33*, 67–73.
- (2) Alanis, A. J. Resistance to Antibiotics: Are We in the Post-Antibiotic Era? *Arch. Med. Res.* **2005**, *36* (6), 697–705. <https://doi.org/10.1016/j.arcmed.2005.06.009>.
- (3) Tünger, Ö.; Dinç, G.; Özbakkaloglu, B.; Atman, Ü. C.; Algün, Ü. Evaluation of Rational Antibiotic Use. *Int. J. Antimicrob. Agents* **2000**, *15* (2), 131–135. [https://doi.org/10.1016/S0924-8579\(00\)00158-8](https://doi.org/10.1016/S0924-8579(00)00158-8).
- (4) Calin, M. A.; Parasca, S. V. Light Sources for Photodynamic Inactivation of Bacteria. *Lasers Med. Sci.* **2009**, *24* (3), 453–460. <https://doi.org/10.1007/s10103-008-0588-5>.
- (5) Fu, X.; Fang, Y.; Yao, M. Antimicrobial Photodynamic Therapy for Methicillin-Resistant *Staphylococcus Aureus* Infection. *Biomed Res. Int.* **2013**, *2013*, 1–9. <https://doi.org/10.1155/2013/159157>.
- (6) DeRosa, M.; Robert J., C. Photosensitized Singlet Oxygen and Its Applications. *Coord. Chem. Rev.* **2002**, *233–234*, 351–371. [https://doi.org/10.1016/S0010-8545\(02\)00034-6](https://doi.org/10.1016/S0010-8545(02)00034-6).
- (7) Kashef, N.; Huang, Y.-Y.; Hamblin, M. R. Advances in Antimicrobial Photodynamic Inactivation at the Nanoscale. *Nanophotonics* **2017**, *6* (5), 853–879. <https://doi.org/10.1515/nanoph-2016-0189>.
- (8) Wainwright, M.; Maisch, T.; Nonell, S.; Plaetzer, K.; Almeida, A.; Tegos, G. P.; Hamblin, M. R. Photoantimicrobials—Are We Afraid of the Light? *Lancet Infect. Dis.* **2017**, *17* (2), e49–e55. [https://doi.org/10.1016/S1473-3099\(16\)30268-7](https://doi.org/10.1016/S1473-3099(16)30268-7).
- (9) Prates, R. A.; Silva, E. G.; Yamada, A. M.; Suzuki, L. C.; Paula, C. R.; Ribeiro, M. S. Light Parameters Influence Cell Viability in Antifungal Photodynamic Therapy in a Fluence and Rate Fluence-Dependent Manner. *Laser Phys.* **2009**, *19* (5), 1038–1044. <https://doi.org/10.1134/S1054660X09050284>.
- (10) Caminos, D. A.; Spesia, M. B.; Pons, P.; Durantini, E. N. Mechanisms of *Escherichia coli* Photodynamic Inactivation by an Amphiphilic Tricationic Porphyrin and 5,10,15,20-Tetra(4-*N,N,N*-Trimethylammoniumphenyl) Porphyrin. *Photochem. Photobiol. Sci.* **2008**, *7* (9), 1071. <https://doi.org/10.1039/b804965c>.
- (11) Marciel, L.; Teles, L.; Moreira, B.; Pacheco, M.; Lourenço, L. M. O.; Neves, M. G. P. M. S.; Tomé, J. P. C.; Faustino, M. A. F.; Almeida, A. An Effective and Potentially Safe Blood Disinfection Protocol Using Tetrapyrrolic Photosensitizers. *Future Med. Chem.* **2017**, *9* (4), 365–379. <https://doi.org/10.4155/fmc-2016-0217>.
- (12) Q. Mesquita, M.; J. Dias, C.; P. M. S. Neves, M.; Almeida, A.; F. Faustino, M. Revisiting Current Photoactive Materials for Antimicrobial Photodynamic Therapy. *Molecules* **2018**, *23* (10), 2424. <https://doi.org/10.3390/molecules23102424>.
- (13) Amin, R. M.; Bhayana, B.; Hamblin, M. R.; Dai, T. Antimicrobial Blue Light Inactivation of *Pseudomonas Aeruginosa* by Photo-Excitation of Endogenous Porphyrins: *In Vitro* and *in Vivo* Studies. *Lasers Surg. Med.* **2016**, *48* (5), 562–568. <https://doi.org/10.1002/lsm.22474>.
- (14) Huang, L.; Wang, M.; Huang, Y.-Y.; El-Hussein, A.; Wolf, L. M.; Chiang, L. Y.; Hamblin, M. R. Progressive Cationic Functionalization of Chlorin Derivatives for Antimicrobial Photodynamic Inactivation and Related Vancomycin Conjugates.

- Photochem. Photobiol. Sci.* **2018**, *17* (5), 638–651. <https://doi.org/10.1039/C7PP00389G>.
- (15) Amos-Tautua, B.; Songca, S.; Oluwafemi, O. Application of Porphyrins in Antibacterial Photodynamic Therapy. *Molecules* **2019**, *24* (13), 2456. <https://doi.org/10.3390/molecules24132456>.
- (16) Almeida-Marrero, V.; Van De Winkel, E.; Anaya-Plaza, E.; Torres, T.; De La Escosura, A. Porphyrinoid Biohybrid Materials as an Emerging Toolbox for Biomedical Light Management. *Chem. Soc. Rev.* **2018**, *47* (19), 7369–7400. <https://doi.org/10.1039/c7cs00554g>.
- (17) Almeida-Marrero, V.; González-Delgado, J. A.; Torres, T. Emerging Perspectives on Applications of Porphyrinoids for Photodynamic Therapy and Photoinactivation of Microorganisms. *Macroheterocycles* **2019**, *12* (1), 8–16. <https://doi.org/10.6060/mhc181220t>.
- (18) Le Guern, F.; Sol, V.; Ouk, C.; Arnoux, P.; Frochot, C.; Ouk, T.-S. Enhanced Photobactericidal and Targeting Properties of a Cationic Porphyrin Following the Attachment of Polymyxin B. *Bioconjug. Chem.* **2017**, *28* (9), 2493–2506. <https://doi.org/10.1021/acs.bioconjchem.7b00516>.
- (19) Žudytė, B.; Lukšienė, Ž. Toward Better Microbial Safety of Wheat Sprouts: Chlorophyllin-Based Photosensitization of Seeds. *Photochem. Photobiol. Sci.* **2019**, *18* (10), 2521–2530. <https://doi.org/10.1039/C9PP00157C>.
- (20) Lourenço, L. M. O.; Sousa, A.; Gomes, M. C.; Faustino, M. A. F.; Almeida, A.; Silva, A. M. S.; Neves, M. G. P. M. S.; Cavaleiro, J. A. S.; Cunha, Â.; Tomé, J. P. C. Inverted Methoxypyridinium Phthalocyanines for PDI of Pathogenic Bacteria. *Photochem. Photobiol. Sci.* **2015**, *14*, 1853–1863.
- (21) Amaral, L. S.; Azevedo, E. B.; Perussi, J. R. The Response Surface Methodology Speeds up the Search for Optimal Parameters in the Photoinactivation of *E. coli* by Photodynamic Therapy. *Photodiagnosis Photodyn. Ther.* **2018**, *22* (February), 26–33. <https://doi.org/10.1016/j.pdpdt.2018.02.020>.
- (22) Tomé, J. P. C.; Neves, M. G. P. M. S.; Tomé, A. C.; Cavaleiro, J. A. S.; Soncin, M.; Magaraggia, M.; Ferro, S.; Jori, G. Synthesis and Antibacterial Activity of New Poly-S-Lysine–Porphyrin Conjugates. *J. Med. Chem.* **2004**, *47* (26), 6649–6652. <https://doi.org/10.1021/jm040802v>.
- (23) Hamblin, M. R.; Hasan, T. Photodynamic Therapy: A New Antimicrobial Approach to Infectious Disease? *Photochem. Photobiol. Sci.* **2004**, *3* (5), 436–450. <https://doi.org/10.1039/b311900a>.
- (24) Alves, E.; Faustino, M. A. F.; Neves, M. G. P. M. S.; Cunha, Â.; Nadais, H.; Almeida, A. Potential Applications of Porphyrins in Photodynamic Inactivation beyond the Medical Scope. *J. Photochem. Photobiol. C Photochem. Rev.* **2015**, *22*, 34–57. <https://doi.org/10.1016/j.jphotochemrev.2014.09.003>.
- (25) Cieplik, F.; Deng, D.; Crielaard, W.; Buchalla, W.; Hellwig, E.; Al-Ahmad, A.; Maisch, T. Antimicrobial Photodynamic Therapy – What We Know and What We Don't. *Crit. Rev. Microbiol.* **2018**, *44* (5), 571–589. <https://doi.org/10.1080/1040841X.2018.1467876>.
- (26) Bonnett, R.; Krysteva, M. A.; Lalov, I. G.; Artarsky, S. V. Water Disinfection Using Photosensitizers Immobilized on Chitosan. *Water Res* **2006**, *40* (6), 1269–1275. <https://doi.org/10.1016/j.watres.2006.01.014>.
- (27) Sabbahi, S.; Alouini, Z.; Ben Ayed, L.; Jemli, M. Inactivation of Faecal Bacteria in Wastewater by Methylene Blue and Visible Light. *Desalin. Water Treat.* **2010**, *20* (1–3), 209–219. <https://doi.org/10.5004/dwt.2010.1171>.
- (28) Pereira, M. A.; Faustino, M. A. F.; Tomé, J. P. C.; Neves, M. G. P. M. S.; Tomé, A. C.; Cavaleiro, J. A. S.; Cunha, Â.; Almeida, A. Influence of External Bacterial Structures on the Efficiency of Photodynamic Inactivation by a Cationic Porphyrin. *Photochem. Photobiol. Sci.* **2014**, *13* (4), 680. <https://doi.org/10.1039/c3pp50408e>.
- (29) Sousa, V.; Gomes, A. T. P. C.; Freitas, A.; Faustino, M. A. F.; Neves, M. G. P. M. S.; Almeida, A. Photodynamic Inactivation of *Candida Albicans* in Blood Plasma and

- Whole Blood. *Antibiotics* **2019**, *8* (4), 221. <https://doi.org/10.3390/antibiotics8040221>.
- (30) Wen, X.; Li, Y.; Hamblin, M. R. Photodynamic Therapy in Dermatology beyond Non-Melanoma Cancer: An Update. *Photodiagnosis Photodyn. Ther.* **2017**, *19*, 140–152.
- (31) Konopka, K.; Goslinski, T. Photodynamic Therapy in Dentistry. *J. Dent. Res.* **2007**, *86* (8), 694–707. <https://doi.org/10.1177/154405910708600803>.
- (32) Diogo, P.; Faustino, M. F. A.; Neves, G. M. P. M. S.; Palma, P. J.; Baptista, I. P.; Gonçalves, T.; Santos, J. M. An Insight into Advanced Approaches for Photosensitizer Optimization in Endodontics—a Critical Review. *J. Funct. Biomater.* **2019**, *10* (4), 44. <https://doi.org/10.3390/jfb10040044>.
- (33) Cruz-Oliveira, C.; Almeida, A. F.; Freire, J. M.; Caruso, M. B.; Morando, M. A.; Ferreira, V. N. S.; Assunção-Miranda, I.; Gomes, A. M. O.; Castanho, M. A. R. B.; Da Poian, A. T. Mechanisms of Vesicular Stomatitis Virus Inactivation by Protoporphyrin IX, Zinc-Protoporphyrin IX, and Mesoporphyrin IX. *Antimicrob. Agents Chemother.* **2017**, *61* (6). <https://doi.org/10.1128/AAC.00053-17>.
- (34) Wiehe, A.; O'Brien, J. M.; Senge, M. O. Trends and Targets in Antiviral Phototherapy. *Photochem. Photobiol. Sci.* **2019**, *18* (11), 2565–2612. <https://doi.org/10.1039/C9PP00211A>.
- (35) Louis, B.; Waikhom, S. D.; Atadja, P. W. Current Trends in Outwitting Resistance Development in Candida Infections through Photodynamic and Short Peptide Therapies: A Strategic-Shift from Conventional Antifungal Agents. *Expert Rev. Anti. Infect. Ther.* **2016**, *14* (3), 345–352. <https://doi.org/10.1586/14787210.2016.1147953>.
- (36) Reinhard, A.; Sandborn, W. J.; Melhem, H.; Bolotine, L.; Chamailard, M.; Peyrin-Biroulet, L. Photodynamic Therapy as a New Treatment Modality for Inflammatory and Infectious Conditions. *Expert Rev. Clin. Immunol.* **2015**, *11* (5), 637–657. <https://doi.org/10.1586/1744666X.2015.1032256>.
- (37) Jori, G.; Brown, S. B. Photosensitized Inactivation of Microorganisms. *Photochem. Photobiol. Sci.* **2004**, *3* (5), 403. <https://doi.org/10.1039/b311904c>.
- (38) Vieira, C.; Gomes, A. T. P. C.; Mesquita, M. Q.; Moura, N. M. M.; Neves, M. G. P. M. S.; Faustino, M. A. F.; Almeida, A. An Insight Into the Potentiation Effect of Potassium Iodide on APDT Efficacy. *Front. Microbiol.* **2018**, *9*, 1–16. <https://doi.org/10.3389/fmicb.2018.02665>.
- (39) Huang, L.; Szewczyk, G.; Sarna, T.; Hamblin, M. R. Potassium Iodide Potentiates Broad-Spectrum Antimicrobial Photodynamic Inactivation Using Photofrin. *ACS Infect. Dis.* **2017**, *3* (4), 320–328. <https://doi.org/10.1021/acsinfecdis.7b00004>.
- (40) Huang, L.; El-Hussein, A.; Xuan, W.; Hamblin, M. R. Potentiation by Potassium Iodide Reveals That the Anionic Porphyrin TPPS4 Is a Surprisingly Effective Photosensitizer for Antimicrobial Photodynamic Inactivation. *J. Photochem. Photobiol. B Biol.* **2018**, *178* (August 2017), 277–286. <https://doi.org/10.1016/j.jphotobiol.2017.10.036>.
- (41) Hamblin, M. R. R. Potentiation of Antimicrobial Photodynamic Inactivation by Inorganic Salts. *Expert Rev. Anti. Infect. Ther.* **2017**, *15* (11), 1059–1069. <https://doi.org/10.1080/14787210.2017.1397512>.
- (42) Huang, L.; Bhayana, B.; Xuan, W.; Sanchez, R. P.; McCulloch, B. J.; Lalwani, S.; Hamblin, M. R. Comparison of Two Functionalized Fullerenes for Antimicrobial Photodynamic Inactivation: Potentiation by Potassium Iodide and Photochemical Mechanisms. *J. Photochem. Photobiol. B Biol.* **2018**, *186*, 197–206. <https://doi.org/10.1016/j.jphotobiol.2018.07.027>.
- (43) Yuan, L.; Lyu, P.; Huang, Y. Y.; Du, N.; Qi, W.; Hamblin, M. R.; Wang, Y. Potassium Iodide Enhances the Photobactericidal Effect of Methylene Blue on *Enterococcus Faecalis* as Planktonic Cells and as Biofilm Infection in Teeth. *J. Photochem. Photobiol. B Biol.* **2020**, *203* (December 2019), 111730. <https://doi.org/10.1016/j.jphotobiol.2019.111730>.
- (44) Vieira, C.; Santos, A.; Mesquita, M. Q.; Gomes, A. T. P. C.; Neves, M. G. P. M. S.; Faustino, M. A. F.; Almeida, A. Advances in APDT Based on the Combination of a Porphyrinic Formulation with Potassium Iodide: Effectiveness on Bacteria and Fungi Planktonic/Biofilm Forms and Viruses. *J. Porphyr. Phthalocyanines* **2019**, *23*, 534–545.

- <https://doi.org/10.1142/S1088424619500408>.
- (45) Branco, T. M.; Valério, N. C.; Jesus, V. I. R.; Dias, C. J.; Neves, M. G. P. M. S.; Faustino, M. A. F.; Almeida, A. Single and Combined Effects of Photodynamic Therapy and Antibiotics to Inactivate *Staphylococcus Aureus* on Skin. *Photodiagnosis Photodyn. Ther.* **2018**, *21* (December 2017), 285–293. <https://doi.org/10.1016/j.pdpdt.2018.01.001>.
- (46) Agazzi, M. L.; Ballatore, M. B.; Reynoso, E.; Quiroga, E. D.; Durantini, E. N. Synthesis, Spectroscopic Properties and Photodynamic Activity of Two Cationic BODIPY Derivatives with Application in the Photoinactivation of Microorganisms. *Eur. J. Med. Chem.* **2017**, *126*, 110–121. <https://doi.org/10.1016/j.ejmech.2016.10.001>.
- (47) Costa, D. C. S.; Gomes, M. C.; Faustino, M. A. F.; Neves, M. G. P. M. S.; Cunha, Â.; Cavaleiro, J. A. S.; Almeida, A.; Tomé, J. P. C. Comparative Photodynamic Inactivation of Antibiotic Resistant Bacteria by First and Second Generation Cationic Photosensitizers. *Photochem. Photobiol. Sci.* **2012**, *11* (12), 1905–1913. <https://doi.org/10.1039/c2pp25113b>.
- (48) Costa, D. C. S.; Pais, V. F.; Silva, A. M. S.; Cavaleiro, J. A. S.; Pischel, U.; Tomé, J. P. C. Cationic Porphyrins with Inverted Pyridinium Groups and Their Fluorescence Properties. *Tetrahedron Lett.* **2014**, *55* (30), 4156–4159. <https://doi.org/10.1016/j.tetlet.2014.05.108>.
- (49) Armarego, W. L. F.; Chai, C. L. L. *Purification of Laboratory Chemicals*, Seventh.; Butterworth-Heinemann, Ed.; Elsevier: Oxford, 2013.
- (50) Kadish, K. M.; Smith, K. M.; Guillard, R. Handbook of Porphyrin Science (Volumes 6 – 10). In *Handbook of Porphyrin Science (With applications to Chemistry, Physics, Materials Science, Engineering, Biology and Medicine)*; Handbook of Porphyrin Science; World Scientific Publishing Company, 2010; Vol. 10, pp 377–390.
- (51) Castro-Olivares, R.; Günther, G.; Zanocco, A. L.; Lemp, E. Linear Free Energy Relationship Analysis of Solvent Effect on Singlet Oxygen Reactions with Mono and Disubstituted Anthracene Derivatives. *J. Photochem. Photobiol. A Chem.* **2009**, *207* (2–3), 160–166. <https://doi.org/10.1016/j.jphotochem.2009.05.012>.
- (52) Prostack, A.; Mark, H. B.; Hansen, W. N. Simultaneous Electrochemical and Internal-Reflection Spectrometric Measurements Using Gold-Film Electrodes. *J. Phys. Chem.* **1968**, *72*, 2576–2582.
- (53) Menezes, J. C. J. M. D. S.; Faustino, M. A. F.; de Oliveira, K. T.; Uliana, M. P.; Ferreira, V. F.; Hackbarth, S.; Röder, B.; Teixeira Tasso, T.; Furuyama, T.; Kobayashi, N.; *et al.* Synthesis of New Chlorin e 6 Trimethyl and Protoporphyrin IX Dimethyl Ester Derivatives and Their Photophysical and Electrochemical Characterizations. *Chem. - A Eur. J.* **2014**, *20* (42), 13644–13655. <https://doi.org/10.1002/chem.201403214>.
- (54) Gomes, M. C.; Woranovicz-Barreira, S. M.; Faustino, M. A. F.; Fernandes, R.; Neves, M. G. P. M. S.; Tomé, A. C.; Gomes, N. C. M.; Almeida, A.; Cavaleiro, J. A. S.; Cunha, Â.; *et al.* Photodynamic Inactivation of *Penicillium Chrysogenum Conidia* by Cationic Porphyrins. *Photochem. Photobiol. Sci.* **2011**, *10* (11), 1735. <https://doi.org/10.1039/c1pp05174a>.
- (55) Ramos, C. I. V.; Marques, M. G. S.; Correia, A. J. F.; Serra, V. V.; Tomé, J. P. C.; Tomé, A. C.; Neves, M. G. P. M. S.; Cavaleiro, J. A. S. Reduction of Cationic Free-Base *Meso*-Tris-*N*-Methylpyridinium-4-Yl Porphyrins in Positive Mode Electrospray Ionization Mass Spectrometry. *J. Am. Soc. Mass Spectrom.* **2007**, *18* (4), 762–768. <https://doi.org/10.1016/j.jasms.2006.12.009>.
- (56) Moura, N. M. M.; Faustino, M. A. F.; Neves, M. G. P. M. S.; Tomé, A. C.; Rakib, E. M.; Hannioui, A.; Mojahidi, S.; Hackbarth, S.; Röder, B.; Paz, F. A. A.; *et al.* Novel Pyrazoline and Pyrazole Porphyrin Derivatives: Synthesis and Photophysical Properties. *Tetrahedron* **2012**, *68* (39), 8181–8193. <https://doi.org/10.1016/j.tet.2012.07.072>.
- (57) Huang, Y. Y.; Choi, H.; Kushida, Y.; Bhayana, B.; Wang, Y.; Hamblin, M. R. Broad-Spectrum Antimicrobial Effects of Photocatalysis Using Titanium Dioxide Nanoparticles Are Strongly Potentiated by Addition of Potassium Iodide. *Antimicrob. Agents Chemother.* **2016**, *60* (9), 5445–5453. <https://doi.org/10.1128/AAC.00980-16>.
- (58) Wen, X.; Zhang, X.; Szewczyk, G.; El-Husseini, A.; Huang, Y.-Y.; Sarna, T.; Hamblin,

- M. R. Potassium Iodide Potentiates Antimicrobial Photodynamic Inactivation Mediated by Rose Bengal in *In Vitro* and *In Vivo* Studies. *Antimicrob. Agents Chemother.* **2017**, *61* (7). <https://doi.org/10.1128/AAC.00467-17>.
- (59) Santos, A. R.; Batista, A. F. P. P.; Gomes, A. T. P. C.; Neves, M. G. P. M. S.; Faustino, M. A. F.; Almeida, A.; Hioka, N.; Mikcha, J. M. G. G. The Remarkable Effect of Potassium Iodide in Eosin and Rose Bengal Photodynamic Action against *Salmonella Typhimurium* and *Staphylococcus Aureus*. *Antibiotics* **2019**, *8* (4), 211. <https://doi.org/10.3390/antibiotics8040211>.
- (60) Simões, C.; Gomes, M. C.; Neves, M. G. P. M. S.; Cunha, Â.; Tomé, J. P. C.; Tomé, A. C.; Cavaleiro, J. A. S.; Almeida, A.; Faustino, M. A. F. Photodynamic Inactivation of *Escherichia coli* with Cationic *Meso*-Tetraarylporphyrins – The Charge Number and Charge Distribution Effects. *Catal. Today* **2016**, *266*, 197–204. <https://doi.org/10.1016/j.cattod.2015.07.031>.

Journal Pre-proof

Highlights

-

PDI with thiopyridyl/pyridinone porphyrins combined with potassium iodide and thiopyridinium/methoxypyridinium porphyrins were effective to photoinactivate *E. coli*.

-

Neutral and cationic porphyrins are able to generate singlet oxygen under white light irradiation.

-

Neutral PSs **1**, **1a**, **2** and **2a** with addition of KI salt show a fast inactivation rate of the Gram-negative bacterium, reaching the detection limit of the method after 5 min of light irradiation.

-

Cationic PSs **1b**, **1c**, **2b** and **2c** at concentration of 5.0 μM promoted a decrease in the viability of *E. coli* till the detection limit of the methodology.

Declaration of interests

The authors declare that they have no known competing financial interests or personal relationships that could have appeared to influence the work reported in this paper.

The authors declare the following financial interests/personal relationships which may be considered as potential competing interests:

All the authors/co-authors declare no conflict of interest.

Journal Pre-proof